Isomorphous Substitution of Iron in the Framework of Zeolite ZSM-23

RAJIV KUMAR AND PAUL RATNASAMY

National Chemical Laboratory, Pune 411 008, India

A crystalline ferrisilicate having the framework structure of ZSM-23 zeolite has been synthesized and characterized. The presence of iron in the zeolite lattice framework has been confirmed by spectroscopic (XRD, framework IR, ESR, and XPS), DTA/TG, magnetic susceptibility, ion exchange, and catalytic activity results. Chemical analysis and XPS show the absence of any significant quantity of $Al(SiO_2/Al_2O_3 > 1400)$ in the ferrisilicate. XRD patterns of the as-synthesized as well as the calcined Fe/ZSM-23 matched well with that of ZSM-23 (MTT topology). Framework IR bands of ZSM-23 are shifted toward lower frequencies on incorporation of iron in the framework. The white color of the as-synthesized as well as that of calcined samples of Fe/ZSM-23, ESR ($g = 4.4$), and magnetic susceptibility ($\mu = 5.4$–5.8, BM) data indicate that Fe–O–Fe interactions (due to oxides of iron like Fe_2O_3 or Fe_3O_4) are absent, and that well dispersed Fe^{3+} ions are present in a magnetically dilute environment. Fe/ZSM-23 exhibits significant ion exchange capacity and catalytic activity/shape selectivity in the metaxylene isomerization reaction. Fe^{3+} ions in zeolite lattice positions account for the ion exchange capacity and shape selective catalytic activity of this crystalline ferrisilicate. © 1990 Academic Press, Inc.

INTRODUCTION

One of the emerging trends in the area of zeolite catalysis is the synthesis and application in catalytic reactions of metallosilicates which contain elements other than aluminium (like B, Fe, Ga) in framework positions (*1*). Since the latter ions possess values of charge/radius ratios different from those of Al^{3+}, the intrinsic acid strength of their associated protons and, hence, their catalytic activity/selectivity may vary on such isomorphous substitution (*2, 3*). Synthesis of novel metallosilicates and investigation of their catalytic properties is, therefore, desirable. The present study reports the synthesis, characterization, and catalytic activity of the iron analog of ZSM-23 containing Fe^{3+} ions in lattice positions. Such a study has not been reported, so far, in the journal literature.

Isomorphous substitution of iron in the MFI framework (ZSM-5 type zeolites) is now well established (*1–4*). The iron analog of sodalite with significant quantities of iron in the framework ($SiO_2/Fe_2O_3 = 6$–30) has been reported by Szostak and Thomas (*5*). A partial replacement of Al^{3+} by Fe^{3+} in the faujasite lattice was achieved recently (*6*) in our laboratory. Very recently, in an Al^{3+}-free system we had synthesized (*7*) a crystalline large pore ferrisilicate with the framework structure of zeolite beta ($SiO_2/Fe_2O_3 = 37$).

ZSM-23 is a medium pore, high silica, zeolite first synthesized by Plank *et al.* (*8*) using pyrrolidine as an organic guest molecule. The framework topology of ZSM-23 (designated as MTT, Mobile-Twenty-Three) is composed of 5-, 6-, and 10-rings with 24 T-atoms per unit cell (*9*). Two other zeolites, namely, KZ-1 (*10*) and ISI-4 (*11*), also possess the MTT framework (*9*). The 10-membered nonintersecting channels of ZSM-23 possess peculiar tear-drop-shaped pore openings of ca. 0.56×0.45 nm. The presence of somewhat narrower pore openings and absence of channel intersections in ZSM-23, vis-a-vis those in ZSM-5, make this zeolite quite interesting from ad-

sorption and catalytic (12–15) points of view. ZSM-23 exhibits shape selectivity different (12–17) than that of ZSM-5.

ZSM-23 can be synthesized using a variety of organic templates such as pyrrolidine (8), heptamethonium bromide (18, 19), octamethomium bromide (19), diisopropanol amine (20), etc. Recently a systematic study of crystallization kinetics of zeolite ZSM-23 has been reported (21). In the present paper a similar synthesis procedure has been adapted, with some modifications, to prepare Fe/ZSM-23. The characterization of this ferrisilicate zeolite was carried out by employing a variety of instrumental methods.

EXPERIMENTAL

Synthesis

Fe/ZSM-23 was synthesized hydrothermally under agitation using fumed silica (Sigma S-5505), pyrrolidine (Fluka), ferric nitrate (GR grade), sodium hydroxide (Analar, grade), and sulfuric acid (98%). In a typical preparation, to 9.9 g of fumed silica were added 105 g of distilled water and 2.7 g NaOH pellets under stirring. This mixture was stirred for 2 h at room temperature (297 K) before adding it to a solution of 1.21 g $Fe(NO_3)_3 \cdot 9H_2O$ in 30 g H_2O very slowly during 30 min. This mixture was stirred for 30 min. Then, 5.4 g pyrrolidine was added slowly to the ferrisilicate mixture. Finally, 2.6 g of H_2SO_4 (98%) was added dropwise under vigorous stirring. The resulting, white gel was then stirred for 15 min before transferring it into a stainless steel autoclave (200 ml capacity). The sealed autoclave was rotated (at 70 rpm) in an oven thermostated at 443 K for 3 days. After the crystallization was complete, the autoclave was removed, and quenched with cold water. The solid contents were filtered, washed thoroughly with deionized water, and dried at 393 K for 8 h. The solid crystalline white material so obtained was calcined in a flow of nitrogen at 733 K for 8 h, and then in air at the same temperature

for an additional 8 h. The heating rate was kept at 1°/min. The organic-free Na form of the ferrisilicate was then ion exchanged with a dilute solution of ammonium hydroxide (the pH of the slurry was kept between 7–8) under reflux to get NH_4–Fe/ZSM-23. This ammonium exchange procedure was repeated twice. The catalytically active protonic form was obtained by calcining the NH_4–Fe/ZSM-23 zeolite at 733 K for 16 h in a flow of dry air. The conventional Al/ZSM-23 was prepared according to published procedures (13, 14, 21).

Characterization

The phase identification and crystallinity determination were carried out by X-ray diffraction (Philips, PW-1710 Cu$K\alpha$). The chemical analyses were carried out by a combination of wet chemical and atomic absorption (Hitachi Z-800) methods. Further characterization of the zeolites was performed by scanning electron microscopy (Cambridge, Stereoscan 150), X-ray photoelectron (Vacuum generators, Mark III), electron spin resonance (Bruker E-2000), and framework IR (Pye Unicam SP3-300, nujol mull technique) spectroscopies. The zeolites were also characterized by thermal analysis, adsorption, magnetic susceptibility, ion exchange, and catalytic methods. The adsorption of normal- and cyclohexanes, and water was carried out gravimetrically using a conventional Mc-Bain balance. The magnetic susceptibility was measured in the range of 94 to 297 K using a Faraday balance (Cahn Ventron USA). The ion exchange properties of Fe/ZSM-23 were evaluated by first saturating the calcined (organic free) ferrisilicate sample with 1.0 N NaCl and then by ion exchanging with potassium. Ion exchange was done under refluxing for 2 h. The procedure was repeated to ensure complete ion exchange. The catalytic activity and selectivity of H-Fe/ZSM-23 were evaluated, using m-xylene isomerization as the test reaction. One gram of the powdered zeolite (14–20 mesh, on dry basis) was

loaded in a tubular downflow silica reactor and the products were analyzed by gas chromatography (Shimadzu) using a 5% bentone-34 + 5% diisodecylphthalate column according to the experimental procedure published earlier (22).

RESULTS AND DISCUSSION

Chemical Composition

The molar oxide composition (by AAS) of calcined Fe/ZSM-23 and Al/ZSM-23 zeolites (on anhydrous basis) was found to be Fe/ZSM-23: 0.7 ± 0.1 Na_2O: Fe_2O_3: 118 ± 1.0 SiO_2 and Al/ZSM-23: 0.8 ± 0.1 Na_2O: Al_2O_3: 109 ± 1.0 SiO_2. Since the silica source was quite pure (fumed silica, S-5505), the Al concentration in the ferrisilicate was found to be negligible ($SiO_2/Al_2O_3 > 1400$); Al could not be detected by XPS either. The color of the as-synthesized as well as that of the calcined, organic-free samples was white. This indicates the absence of the brown iron oxides, at least in the bulk, outside the zeolite crystals.

X-ray Diffraction

The X-ray diffraction patterns of as-synthesized Al/ZSM-23, Fe/ZSM-23, and calcined Fe/ZSM-23 samples are given in Fig. 1, curves A, B, and C, respectively. The XRD patterns of both Al/ZSM-23 and Fe/ZSM-23 matched well with those of MTT zeolites published earlier (9, 10, 13).

Here it may be pertinent to mention that the use of pyrrolidine as the organic guest molecule has not yet resulted in the synthesis of the silica polymorph of ZSM-23. In fact, even carefully optimized synthesis procedures (13, 21) could not produce highly crystalline, pure ZSM-23 having $SiO_2/Al_2O_3 > 150$. Even patent claims (8) for ZSM-23 using pyrrolidine as template are restricted to a SiO_2/Al_2O_3 value below 250. In the absence of Al or Fe salts during ZSM-23 synthesis only cristobalite was obtained. Hence, the Fe/ZSM-23 synthesized in the present study using pyrrolidine in the Al-free system but containing Fe is unlikely to be the pure silica polymorph of ZSM-23, but its ferrisilicate analog.

Scanning Electron Microscopy

Figure 2 shows the scanning electron micrograph of the as-synthesized Fe/ZSM-23. The crystals of Fe/ZSM-23 are in the form of bundles of needles, a typical morphology of ZSM-23 (13, 21), the individual needle being 2–3 μm long and 0.1–0.2 μm thick (from a scan of about 100 crystals). The SEM photograph also confirms the absence of amorphous material *outside* the zeolite crystals.

Thermal Analysis

Figure 3 depicts the thermal behavior (DTA/TG) of as-synthesized Al/ZSM-23 and Fe/ZSM-23 (curves A and B, respectively). There are three main regions of weight loss; the first one around 453 K is due to the loss of water. The other two around 643 and 693–713 K, respectively, are due to the decomposition of organic matter. The first minor exothermic peak around 643 K exhibited by both Fe/ZSM-23 and Al/ZSM-23 samples is probably due to the oxidative decomposition of occluded pyrrolidine. The other exothermic peak around 693 K (in the case of Fe/ZSM-23) or around 713 K (in the case of Al/ZSM-23) may be attributed to the oxidative decomposition of pyrrolidine in intimate interaction with the zeolite framework. This latter species is held less strongly in Fe/ZSM-23 than in the Al analog, causing the observed shift to lower temperature. A similar shift (to lower temperatures) in other ferrisilicate zeolite systems had also been observed earlier on isomorphous substitution of Al by Fe in framework positions (2, 6, 7, 23).

Framework IR Spectroscopy

In Fig. 4 the framework infrared spectra (in the region of 200–1300 cm^{-1}) of the as-synthesized samples of Fe/ZSM-23 and Al/ZSM-23 are compared. In Fe/ZSM-23, in accordance with expectations, most of the lattice vibration bands are shifted to
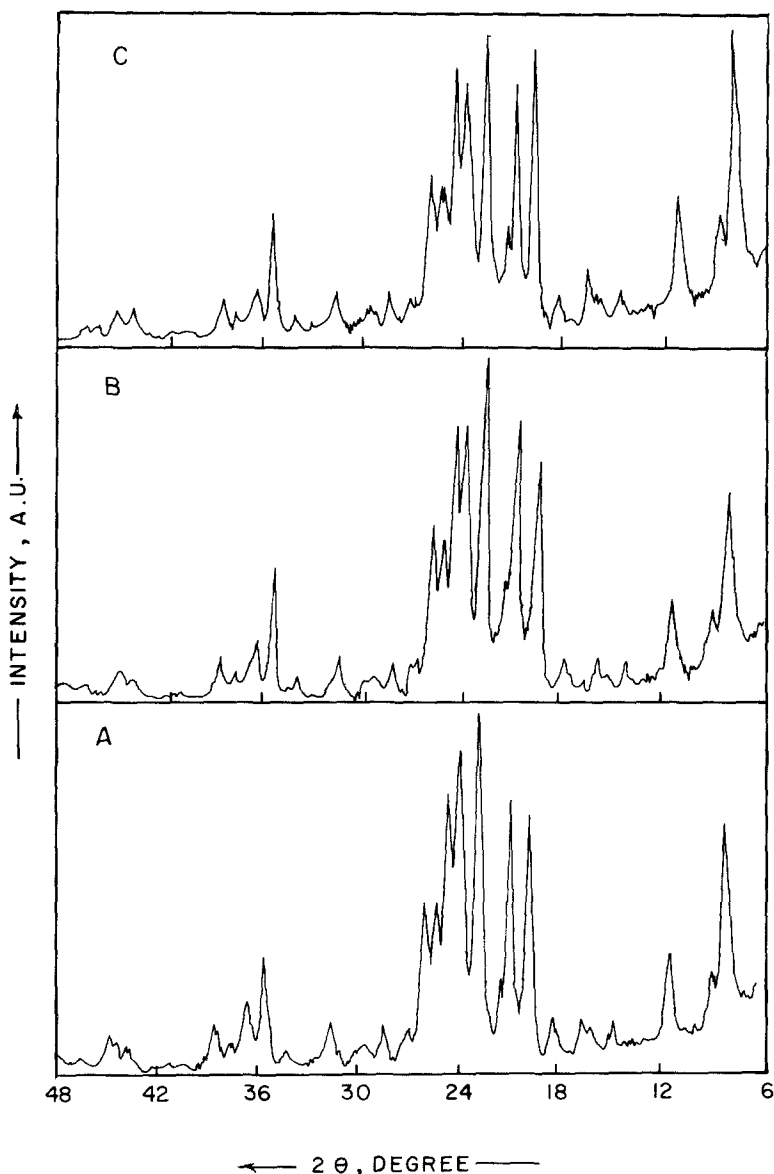
FIG. 1. X-ray powder diffractograms of (A) as-synthesized Al/ZSM-23, (B) as-synthesized Fe/ZSM-23, and (C) calcined Fe/ZSM-23.

lower wave numbers (in comparison with the Al analog, Fig. 4).

ESR Spectroscopy

Though an ESR signal around $g = 4.3–4.4$ cannot be used to confirm the presence of iron in the lattice positions (24), its observation is a necessary consequence of such a presence. The ESR spectrum of the as-synthesized Fe/ZSM-23 sample (Fig. 5) exhibits two main signals at $g = 4.4$ and $g = 2.0$, respectively. The former is assigned to Fe^{3+} in distorted tetrahedral positions possibly in the zeolite lattice.

Magnetic Susceptibility

Magnetic susceptibility measurements can indicate whether the iron is present in a
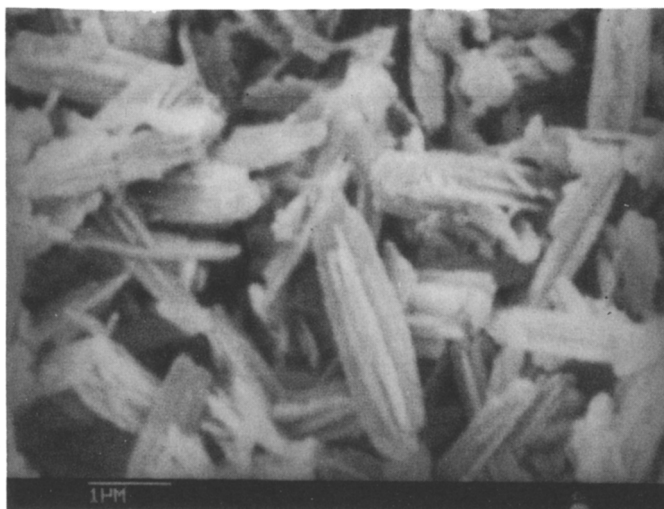
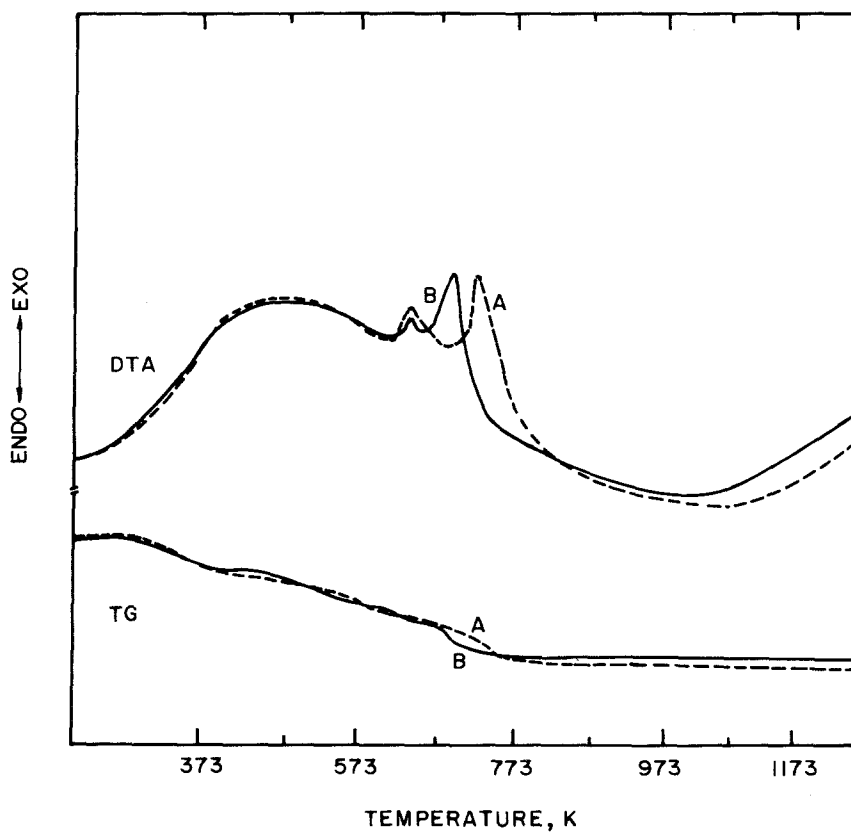FIG. 2. Scanning electron micrograph of as-synthesized Fe/ZSM-23.

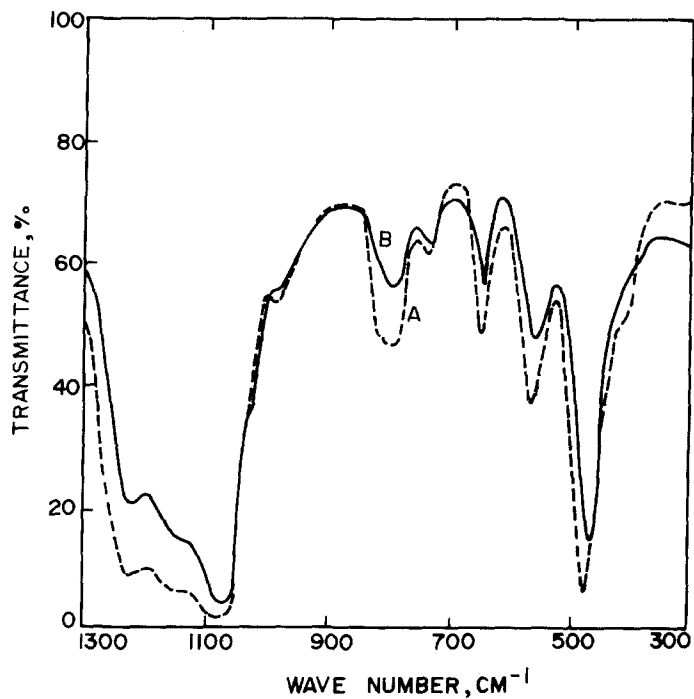FIG. 3. DTA/TG of (A) Al/ZSM-23 and (B) Fe/ZSM-23.

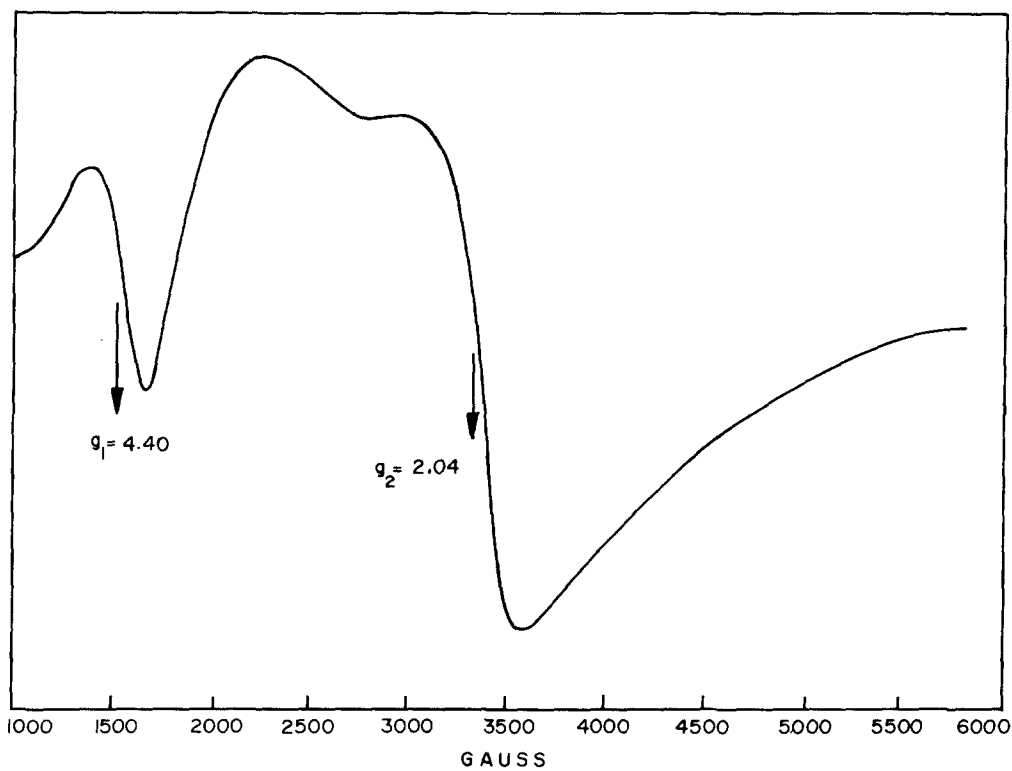FIG. 4. Framework IR of (A) Al/ZSM-23 and (B) Fe/ZSM-23.

FIG. 5. ESR spectrum of Fe/ZSM-23.

magnetically dilute environment (with Si–O–Fe–O–Si bonds) or in a condensed iron oxide phase (with Fe–O–Fe bonds). Noninteracting Fe^{3+} ions in a diamagnetic matrix are expected to have a magnetic moment below about 6 BM. The values of magnetic moments of samples, measured by the Faraday balance method, at 94 and 297 K were found to be 5.7 and 5.4 BM respectively for the as-synthesized Fe/ZSM-23, and 5.8 and 5.6 BM for the protonic form. In the case of high silica ferrisilicate zeolites, the framework Fe^{3+} ions are present in a magnetically dilute environment, and thus should have a magnetic moment below 6 BM. Iron oxides, such as Fe_2O_3 or Fe_3O_4, if present, are expected to exhibit much higher values of the magnetic moment as well as a marked dependence on temperature, depending upon the degree of agglomeration of the iron oxide phase (4, 5). Thus the magnetic susceptibility data confirm that Fe/ZSM-23 does not contain iron oxide phases like Fe_2O_3 or Fe_3O_4, at least in bulk, and that Fe^{3+}–O–Fe^{3+} bonds are absent in it. Aggregates of iron oxide in size greater than about 1 nm would have been detected by this technique if present in more than 0.1% (wt) concentration.

X-ray Photoelectron Spectroscopy

X-ray photoelectron spectrum of the as-synthesized Fe/ZSM-23 sample did not reveal the presence of aluminum. Aluminum, in more than 0.1% (wt) concentration would have been detected in our XPS experiments. Further the oxygen peak was found to be symmetric (Fig. 6), indicating that all the oxygen atoms are present only as the zeolitic lattice oxygen and other discrete phases (like Fe_2O_3, Fe_3O_4, etc.) are absent. The latter phases, when present, exhibit a shoulder in the oxygen peak (2).

Adsorption Studies

The adsorption capacities of the calcined, Na form of ferri-ZSM-23 (Na–Fe/ZSM-23) for n-hexane, cyclohexane, and water are 8.5, 3.5, and 5.8% (wt.), respec-
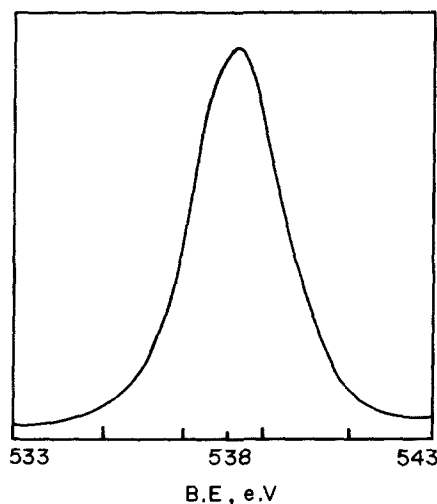

Fig. 6. Oxygen peak in the X-ray photoelectron spectrum of Fe/ZSM-23.

tively, at $P/P_0 = 0.5$ and 297 K. The corresponding adsorption volumes of Al/ZSM-23 ($SiO_2/Al_2O_3 = 109$) for n-hexane, cyclohexane, and water (at $P/P_0 = 0.5$ and 297 K) were found earlier (14) to be 6.4, 2.1, and 4.3, respectively. These adsorption results clearly demonstrate the absence of a significant quantity of any amorphous material occluded *within* the zeolite crystals.

Ion Exchange Properties

After saturating the calcined Fe/ZSM-23 with Na^+, the molar ratio Na/Fe in solid Fe/ZSM-23 was found to be 0.90. On ion exchange of Na–Fe/ZSM-23 with potassium, the molar ratio of K/Fe in the resultant sample was found to be 0.86. The ion exchange property of zeolites is due to tetrahedral MO_4^- groups (M = Al, Fe, etc.) in the framework. Recently Szostak and Thomas (4, 5) have demonstrated that the ion exchange capacities of ferrisilicates can be taken as convincing evidence for the presence of Fe^{3+} in framework positions in the zeolite lattices. Hence, the substantial ion exchange capacity of the calcined Fe/ZSM-23 sample, observed in the present study, provides strong evidence for the presence of most of the Fe^{3+} ions in the

ZSM-23 lattice framework. Based upon the ion exchange capacities of calcined Fe/ZSM-23 for Na (Na/Fe = 0.9, mole ratio) it can be calculated that the upper limit of nonframework iron, if any, is not more than 10 mole% of total iron present in the zeolite.

Catalytic Properties

Metaxylene conversion over the acid form of zeolites provides a wealth of information on the pore geometry and shape selective properties of zeolites (26, 27). It has been found (27) that the ortho-xylene/para-xylene ratio (OX/PX), in the products of metaxylene conversion, is quite sensitive to the subtle differences in the shape and size of the pore openings of various 10-ring medium pore zeolites. A decrease in the value of the OX/PX ratio indicates an increase in the product shape selectivity of the zeolites. The product shape selectivity decreases along the series of 10-ring medium pore zeolites: ZSM-23 > ZSM-48 > ZSM-50 > ZSM-5. The isomerization/disproportionation (I/D) ratio (26) or selectivity for isomerization (Sel. Isom.) (27), based upon restricted transition state shape selectivity, decreases (27) along the series: ZSM-23 > ZSM-48 > ZSM-5 > ZSM-50.

The isomorphous substitution of framework Al by Fe is not expected to alter the shape selective properties, particularly of high silica zeolites. If there is an increase in the shape selectivity (i.e., a decrease in the OX/PX ratio in metaxylene isomerization reaction) on framework isomorphous substitution of Al by Fe, it indicates that a significant part of Fe is present as nonframework occluded material in the zeolite pores, thus reducing the effective pore width. The activity of ferrisilicate zeolites in the proton (Brønsted acid) catalyzed reaction (such as metaxylene conversion) is, however, expected to be lower compared to that of the Al analog because of the lower strength of the Brønsted acid sites associated with the framework Fe in the former (28).

In the present paper a comparison of the activity and shape selectivity of Al/ZSM-23 and Fe/ZSM-23 is made. Table 1 shows the results obtained in the isomerization of m-xylene, a typical Brønsted acid catalyzed reaction (24), over H-Fe/ZSM-23 and H-Al/ZSM-23. The ortho-/para-xylene ratio, an indicator of product shape selectivity, is around 0.27 ± 0.03 for both zeolites. The selectivity for isomerization (14, 27) (equal to (p-xylene + o-xylene)/m-xylene converted), an indicator of transition state shape selectivity, is also similar for both the zeolites, indicating that they possess similar product, as well as transition state, shape selectivities. The two zeolites, however, differ in their activity level at a given reaction condition. The activity of H-Fe/ZSM-23 is lower than that of the Al analog (Table 1). Since the active Brønsted acid sites could have been generated only by protons associated with the framework Fe^{3+} (particularly when Al^{3+} is almost absent, $SiO_2/Al_2O_3 > 1400$), the considerable activity and shape selectivity exhibited by Fe/ZSM-23 provide additional strong evidence for the incorporation of iron in the MTT framework. The lower activity of the iron analog (compared to Al/ZSM-23) arises from the lower strength of acid sites associated with framework iron (28). This feature of the ferrisilicate zeolites makes them attractive catalysts for those reactions which do not require strong acid sites.

CONCLUSIONS

A white crystalline ferrisilicate ($SiO_2/Fe_2O_3 = 118$) with the framework structure of zeolite ZSM-23 has been synthesized. Chemical analysis and XPS confirm that the sample is substantially free of Al. Scanning electron microscopy and adsorption measurements indicate the absence of amorphous matter, both outside the zeolite crystals and within their pore system. The lattice vibration frequencies in the IR region are shifted (relative to those in the Al/ZSM-23) to lower wave numbers due to the presence of the heavier Fe ions. The mate-

TABLE 1

Isomerization of Metaxylene over Fe/ZSM-23 and Al/ZSM-23[a]

Feed: m–Xylene + H_2 (1 : 4, mole)
WHSV: 3.5 h^{-1}
Pressure: Atmospheric

| Temp. (K) | 623 | | 663 | | 683 | | 703 | |
Zeolite	Al	Fe	Al	Fe	Al	Fe	Al	Fe
Conv. (%, wt)	10.2	5.0	18.2	8.0	22.7	12.0	28.2	19.6
Products (%, wt)								
Toluene	0.2	0.1	0.2	0.2	0.3	0.2	0.5	0.4
p-Xylene	7.9	3.9	14.3	6.1	17.9	9.1	21.0	14.4
m-Xylene	89.8	95.0	81.8	92.0	77.3	88.0	71.8	80.4
o-Xylene	2.0	1.0	3.4	1.7	4.2	2.6	6.4	4.4
1,3,5TMB[b]	—	—	0.1	—	0.1	—	0.1	0.1
1,2,4TMB	0.1	—	0.1	—	0.2	0.1	0.2	0.2
1,2,3TMB	—	—	—	—	—	—	—	—
Sel. Isom.[c]	0.97	0.98	0.97	0.97	0.97	0.97	0.97	0.96
o-Xylene/p-xylene	0.25	0.26	0.24	0.28	0.24	0.28	0.30	0.30

[a] Data for Al/ZSM-23 have been taken from Ref. (14) for comparison.

[b] TMB, Trimethylbenzene.

[c] Sel. Isom., (o-xylene + p-xylene)/m-xylene converted.

rial possesses significant ion exchange capacity (Na/Fe = 0.9, K/Fe = 0.86) and exhibits activity and shape selectivity in the isomerization of m-xylene. While magnetic susceptibility data (μ = 5.4–5.8 BM) confirm that the Fe^{3+} ions in the sample are in a magnetically dilute environment (no Fe–O–Fe bonds), the ESR results (g = 4.4) indicate that they are surrounded by four oxide ions at the corners of a distorted tetrahedron. In view of all the above evidence, it is concluded that the material synthesized is indeed the ferrisilicate analog of ZSM-23 containing Fe^{3+} isomorphously substituted for Al^{3+} in framework positions. Even though Fe/ZSM-23 has the same shape selectivity as that of Al/ZSM-23, the former possesses acidic sites weaker than those of the latter and, hence, is of interest in those catalytic reactions which do not require strong acid sites.

REFERENCES

1. Barrer, R. M., "Hydrothermal Chemistry of Zeolites," p. 251. Academic Press, London/New York, 1982.

2. (a) Ratnasamy, P., Borade, R. B., Sivashankar, S., Shiralkar, V. P. and Hegde, S. G., in "Proceedings, Int. Symp. on Zeolite Catalysis, Siofok Hungary, 1985," p. 137; (b) Borade, R. B., Zeolites 7, 398 (1987).

3. Ball, W. J., Dwyer, J., Garforth, A. A., and Smith, W. J., in "Proceedings, 7th Int. Zeolite Conf., Tokyo, 1986," Stud. Surf. Sci. and Catal, 1986, Vol. 28, p. 137. Elsevier, Amsterdam, 1986.

4. Szostak, R., and Thomas, T. L., J. Catal. 100, 555 (1986).

5. Szostak, R., and Thomas, T. L., J. Chem. Soc. Chem. Commun., 113 (1986).

6. Ratnasamy, P., Kotasthane, A. N., Shiralkar, V. P., Thangaraj, A., and Ganapathy, S., Paper presented at the ACS Symposium on "Advances in Zeolite Synthesis," Los Angeles, CA, Sept. 25–27, 1988.

7. Kumar, R., Thangaraj, A., and Ratnasamy, P., Zeolites, in press.

8. Plank, C. J., Rosinski, E. J., and Rubin, M. K., U. S. Patent: 4 076 842 (1978) assigned to Mobil Oil Corp.

9. Rohrman, A. C., Jr., La Pierre, R. B., Schlenker, J. L., Wood, J. D., Valyocsik, E. W., Rubin,

M. K., Higgins, J. B., and Rohrbaugh, W. J., *Zeolites* **5,** 352 (1985).

10. Parker, L. M., and Bibby, D. M., *Zeolites* **3,** 8 (1983).

11. Takatu, K., and Kawata, N., Europ. Patent Appl. 102 467 (1984).

12. Ernst, S., Kokotailo, G. T., Kumar, R., and Weitkamp, J., *in* "Proceedings, 9th International Congress on Catalysis, Calgary, 1988" (M. J. Phillips and M. Ternan, Eds.), p. 389. Chem. Institute of Canada, Ottawa.

13. Ernst, S., Kumar, R., and Weitkamp. J., *Catal. Today* **3,** 1 (1988).

14. Kumar, R., and Ratnasamy, P., *J. Catal.* **116,** 440 (1989).

15. Wu, E. L., Landolt, G. R., Chester, A. W., *in* "Proceedings, 7th Int. Zeolite Conf., Tokyo, 1986," Stud. Surf. Sci. and Catal., Vol. 28, p. 547. Elsevier, Amsterdam, 1986.

16. Bendoraitis, J. G., Chester, A. W., Dwyer, F. G., and Garwood, W. E., *in* "Proceedings, 7th Int. Zeolite Conf., Tokyo, 1986," Stud. Surf. Sci. and Catal., Vol. 28, p. 669. Elsevier, Amsterdam, 1986.

17. Kresge, C. T., Nicoletti, M. P., and Vartuli, J. C., Eur. Pat. Appl. EPA 136 133 (1985) assigned to Mobil Oil Corp.

18. Valyoscik, E. W., U.S. Patent 4 490 342 (1984) assigned to Mobil Oil Corp.

19. Casci, J. L., *in* "Proceedings, 7th Int. Zeolite Conf., Tokyo, 1986," Stud. Surf. Sci. and Catal., Vol. 28, p. 215. Elsevier, Amsterdam, 1986.

20. Barri, S. A. I., U K Patent Appl. G B 2 190 910 A (1987).

21. Ernst, S., Kumar, R., and Weitkamp, J., *in* ACS Symposium Series 398, "Zeolite Synthesis" (M. L. Occelli and H. E. Robson, Eds.), chap. 38, p. 560. American Chemical Society, Washington, DC, 1989.

22. Babu, G. P., Kulkarni, S. B., and Ratnasamy, P., *J. Catal.* **79,** 215 (1983).

23. Kofke, T. J. G., Gorte, R. J., and Kokotailo, G. T., *J. Catal.* **116,** 252 (1989).

24. Kuchirov, A. V., and Slinkin, A. A., *Zeolites* **8,** 10 (1988).

25. Benslama, R., Fraissard, J., Albizane, A., Fajula, F., and Figueras, F., *Zeolites* **8,** 196 (1988).

26. Martens, J. A., Perez-Pariente, J., Sastre, E., Corma, A., and Jacobs, P. A., *Appl. Catal.* **45,** 85 (1989).

27. Kumar, R., Rao, G. N., and Ratnasamy, P., *in* "Proceedings, 8th Int. Zeolite Conf., Amsterdam, July 10–14, 1989," Stud. Surf. Sci. and Catal. (P. A. Jacobs and R. A. Van Santen, Eds.), Vol. 49, p. 1141. Elsevier, Amsterdam, 1989.

28. Chu, C. T. W., and Chang, C. D., *J. Phys. Chem.* **89,** 1569 (1989).